



Cite this: *Analyst*, 2025, **150**, 5142

Received 11th August 2025,  
Accepted 6th October 2025

DOI: 10.1039/d5an00859j

rsc.li/analyst

## Hypochlorite-activated analyte-replacement fluorogenic probes for minute-level fast detection of acute kidney injury

Tingfei Xie,<sup>a,b</sup> Jiahui Chen,<sup>a</sup> Xiaolu Sui,<sup>a</sup> Yanzi Zhang,<sup>a</sup> Jiqiang Liu,<sup>b</sup> Jinxin Zhang,<sup>a,b</sup> Xuechuan Hong,<sup>b</sup> Daoyong Jiang,<sup>a,c</sup> Pengfei Zhang<sup>b</sup> and Jihong Chen<sup>a</sup>

Acute kidney injury (AKI) is a serious condition characterized by high morbidity and mortality, often manifesting as abnormal levels of bioactive molecules such as hypochlorous acid (HClO) in urine. We developed a highly sensitive fluorescent probe, Cy-PITC, capable of selectively lighting up trace hypochlorite at the ppb level in urine. Using this approach, HClO produced in an AKI cell model was sensitively detected. Notably, a significant signal enhancement was observed in the urine of AKI mice compared with the control group. Finally, urine samples from healthy volunteers and AKI patients were clearly distinguished within less than two minutes, without the need for complex instruments or specialized training. This strategy demonstrates great potential for use in low-resource settings, such as households, rural clinics, and conflict zones.

Acute kidney injury (AKI) is a prevalent critical illness in clinical practice, noted for its high incidence, mortality rates, and significant economic impact.<sup>1</sup> The ultra-fast diagnosis of AKI at the early stage can improve the success rate of treatment and reduce the rates of disability and mortality in patients.<sup>2</sup> Current clinical diagnosis of AKI primarily relies on serum

creatinine levels and urine output, as established by KDIGO guidelines, though these indicators often lag 24–48 hours behind actual renal injury. Emerging biomarkers such as KIM-1, NGAL, IL-18, cystatin C, and HClO are under investigation for their potential to enable earlier detection. Current standard clinical procedures for AKI detection are mainly based on pain-inducing invasive blood collection and carried out by professional operators using complex equipment, which makes them unsuitable for frequent surveillance of patients in resource-limited environments (such as homes, battlefields, rural areas, *etc.*).<sup>3–5</sup> Therefore, it is highly desirable to develop non-invasive, cost-effective AKI detection methods with ease of operation, short analysis time, and high sensitivity.

Fluorescence-based biosensing has emerged as a transformative platform for disease monitoring, offering unparalleled advantages in sensitivity, rapidity, and operational simplicity.<sup>6</sup> Researchers have developed various kinds of fluorescent probes for AKI detection and imaging based on different designs.<sup>7–9</sup> Unfortunately, most of them involve intravenous injection followed by *in vivo* imaging, which makes them difficult to be used in clinical AKI patients (as they require very strict ethical reviews and drug clinical trials).<sup>10</sup> Notably, Pu pioneered a urinary nano-sensor achieving non-invasive diagnosis of liver transplant rejection, highlighting the untapped potential of urine-based fluorescence diagnostics for visceral organ injuries (non-invasive nature, abundance, and ease of collection).<sup>11</sup>

Hypochlorous acid (HClO) represents a compelling candidate for AKI biomarker discovery due to its spatiotemporally restricted generation profile and quantifiable urinary excretion. During AKI initiation, renal myeloperoxidase (MPO) undergoes compartmentalized activation in the proximal tubular mitochondria, triggering transient HClO bursts, a pattern distinct from the sustained low-level HClO production observed in systemic inflammation (*e.g.*, rheumatoid arthritis and sepsis). Crucially, HClO's small molecular weight (MW 56) facilitates glomerular filtration into urine,

<sup>a</sup>Department of Nephrology, The People's Hospital of Baoan Shenzhen, The Second Affiliated Hospital of Shenzhen University, Shenzhen Hospital of Guangdong Provincial People's Hospital, Shenzhen School of Clinical Medicine, Southern Medical University, Shenzhen Baoan Clinical Medical School of Guangdong Medical University, The 8th people's Hospital of Shenzhen, Baoan Clinical Research Center for Kidney Disease, Guangdong 518000, PR China.

E-mail: chenjihong0606@hotmail.com

<sup>b</sup>Guangdong Key Laboratory of Nanomedicine, Chinese Academy of Sciences-Hong Kong Joint Lab for Biomaterials, Chinese Academy of Sciences Key Laboratory of Biomedical Imaging Science and System, Shenzhen Key Laboratory of Metabolic Health, Shenzhen Metabolism and Reproductive Targeted Delivery Proof-of-Concept Center, Institute of Biomedicine and Biotechnology, Shenzhen Institutes of Advanced Technology (SIAT), Chinese Academy of Sciences (CAS), Shenzhen, 518055, PR China. E-mail: pf.zhang@siat.ac.cn

<sup>c</sup>School of Chemistry and Life Sciences, Guilin Normal University, Guilin, Guangxi 541199, PR China

<sup>d</sup>Department of Cardiology, Zhongnan Hospital of Wuhan University, School of Pharmaceutical Sciences, Wuhan University, Wuhan, 430071, China



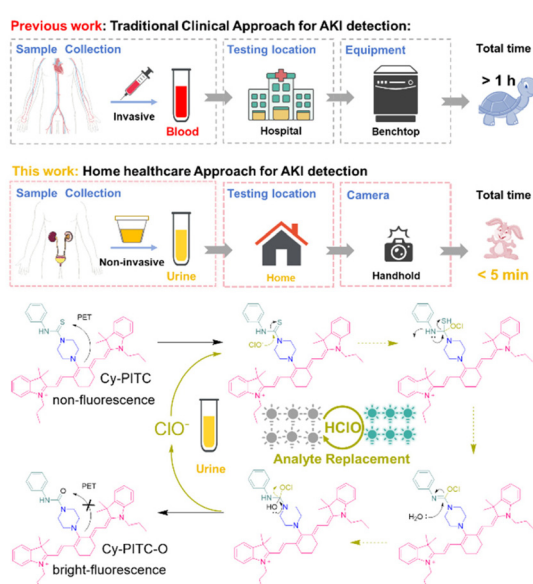
circumventing the protein-binding interference common to larger biomarkers.<sup>12,13</sup> Despite these merits, existing HClO detection methods (electrochemical, chemiluminescent) suffer from poor temporal resolution and matrix.<sup>14</sup>

Herein, we report a near-infrared (NIR) fluorogenic probe (Cy-PITC) engineered for ultrafast (<5 s), selective urinary HClO detection. By conjugating a heptamethine cyanine scaffold with phenyl isothiocyanate (PITC) *via* a piperazine linker, Cy-PITC achieves analyte-specific fluorescence activation through HClO-mediated thiourea oxidation. This design confers two key advantages: (1) NIR emission minimizes background autofluorescence and (2) sub-second reactivity enables real-time tracking of transient HClO surges. Our clinical validation in 30 AKI patients demonstrates robust correlation between the urinary Cy-PITC signal and AKI progression stages, outperforming serum creatinine in temporal resolution by 12–24 hours (Scheme 1).

The synthesis route and structural characterization of Cy-PITC were confirmed using <sup>1</sup>H NMR, <sup>13</sup>C NMR, and MS (Fig. S1–S4). As illustrated in Scheme 1, the sensing mechanism of Cy-PITC involves HClO-specific oxidation of its thiourea group to urea, restoring the conjugated  $\pi$ -system of the heptamethine cyanine fluorophore and activating NIR fluorescence at 798 nm, which was verified through HRMS and theoretical calculations (Fig. S5–S8 and Table S1). UV-vis spectroscopy revealed a maximum absorption peak at 700 nm, significantly reducing background interference in biological matrices (Fig. S9). To validate the diagnostic reliability of Cy-PITC in complex biological matrices, we systematically assessed its performance. In 50% diluted human urine buffer, Cy-PITC exhibited superior selectivity toward ClO<sup>−</sup> over com-

peting ROS (Fig. S10). Cy-PITC exhibited a linear response ( $R^2 = 0.997$ ) with a detection limit of 0.517  $\mu$ M (LOD,  $3\sigma/S$ ) and achieved reaction equilibrium within 1 s, outperforming existing probes which require 1–20 min (ref. 14) (Fig. 1A–C). The fluorescence quantum yield value of Cy-PITC was determined to be 0.0988 using ICG as the standard, which is nearly 76-fold that of Cy-PITC solution ( $\Phi = 0.0013$ ) at 798 nm. The probe demonstrated exceptional selectivity, showing <5% signal variation toward 8 potential interferents including AKI biomarkers (NGAL, IL-18), urinary metabolites (creatinine, urea), other renal disease-specific markers (human albumin, glucose), and urinary electrolytes (NaCl, KCl) (Fig. 1D and S11). Robust performance was maintained across physiological urine pH (4.6–8.0)<sup>15</sup> with 50% activity retention (Fig. S12). Cy-PITC sets itself apart from existing reaction-based ClO<sup>−</sup>/HClO probes, coupled with ultrafast kinetics and impressive sensitivity (Table S2).

To further evaluate the potential application of Cy-PITC for cell imaging, human kidney 2 (HK-2) cells were incubated with Cy-PITC and imaged with a confocal fluorescence microscope. Cy-PITC demonstrated excellent biosafety, with no significant cytotoxicity observed in HK-2 cells after 24 h of exposure (Fig. S13). Cy-PITC's capacity for reporting AKI-associated oxidative stress was assessed and it was found that cisplatin-treated cells (a well-established AKI model)<sup>16</sup> and exogenous ClO<sup>17</sup> stimulated cells both exhibited intense cytoplasmic NIR fluorescence upon Cy-PITC incubation, confirming probe activation under pathological ROS conditions (Fig. 2 and S14). Notably, *N*-acetylcysteine (NAC) pretreatment attenuated the NIRF signal by 72%, consistent with NAC's ROS-scavenging mechanism *via* glutathione synthesis.<sup>18</sup> This pharmacological



**Scheme 1** Design and advantages of Cy-PITC for non-invasive, point-of-care AKI detection. Utilizing urine samples, Cy-PITC enables non-invasive early AKI diagnosis by triggering NIR fluorescence within 5 seconds, facilitating portable home-based testing.

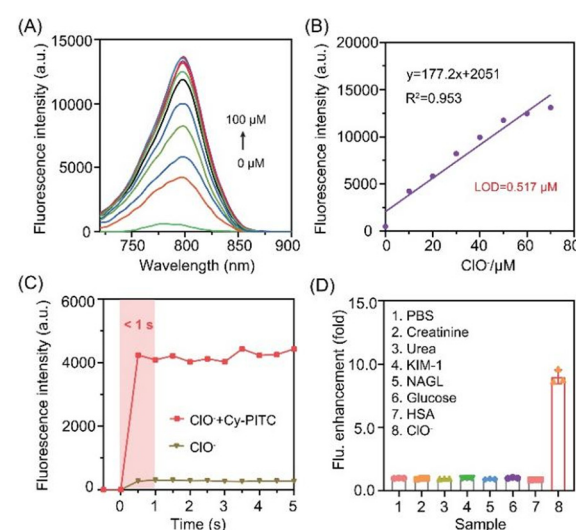


**Fig. 1** (A) The alteration of fluorescence intensity of Cy-PITC (1  $\mu$ M in 50% diluted human urine buffer) upon addition of increasing amounts of HClO/ClO<sup>−</sup>. (B) The linear relationship between the peak fluorescence intensity and the HClO/ClO<sup>−</sup> concentration. (C) The fluorescence intensity from 0 to 5 seconds, after the introduction of Cy-PITC (1  $\mu$ M) into HClO/ClO<sup>−</sup> (100  $\mu$ M). (D) Fluorescence spectra of the reaction of Cy-PITC with HClO/ClO<sup>−</sup> and other various analytes.



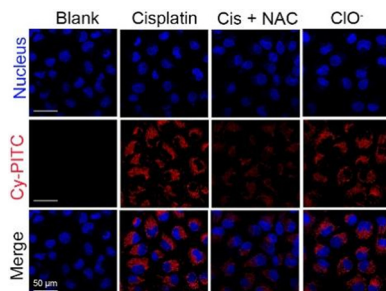


**Fig. 2** Fluorescence image of Cy-PITC (2  $\mu$ M) in HK-2 cells. Cis = cisplatin.

rescue effect correlated with reduced cisplatin-induced tubular damage (Fig. S15), validating Cy-PITC's responsiveness to dynamic redox changes during AKI progression.

Cy-PITC was then used to image cisplatin-induced AKI in a mouse model. Fluorescence changes in the kidneys were determined at different times after injection of Cy-PITC (100  $\mu$ L, 0.2 mM) through the tail vein of mice 24 h or 48 h after intraperitoneal injection of cisplatin (20 mg kg<sup>-1</sup>). As shown in Fig. 3A, the fluorescence intensity in the kidneys increased time-dependently during 60 min and remained stable until 120 min. The kidneys of mice pretreated with cisplatin, followed by intravenous injection of Cy-PITC, exhibited fluorescence enhancement compared to the control group. The fluorescence of the main organs was unchanged after the injection of Cy-PITC in the control mice. Major organs were collected from mice for fluorescence imaging. As shown in Fig. 3B, the fluorescence signal increases with increasing cisplatin duration. A significant difference in fluorescence signal intensity was observed in the kidneys at 24 h and 48 h after cisplatin injection compared to the control group. At the same time, we also saw an increase in the fluorescence signal in the liver, which is related to oxidative stress in the liver caused by cisplatin. This suggests that the enhanced fluorescence signal of HClO in cisplatin-induced drug models is not unique to the kidneys. This indicates that urine sample imaging is a more

specific and preferable option in cisplatin-induced AKI models.

Thus, we evaluated Cy-PITC's diagnostic utility in urine specimens (Fig. 4A). Urine from healthy controls displayed negligible fluorescence, whereas AKI samples generated intense signals with a 5-fold fluorescence enhancement *versus* controls (Fig. 4B and S16). To assess early detection capability, longitudinal monitoring at 0/24/48 h post-cisplatin treatment revealed a 3.3-fold fluorescence increase at 24 h prior to detectable serum creatinine elevation (Fig. S17) increasing to 5.3-fold at 48 h (Fig. 4C). Importantly, the Cy-PITC fluorescence intensity exhibited a positive correlation with histopathological injury scores (Fig. 4D), demonstrating its capacity to quantify AKI severity. This further confirms Cy-PITC's ability to identify renal compromise earlier than creatinine-based assays, attributable to renal functional reserve masking early-stage serum creatinine changes.<sup>19</sup> Compared to existing urinary imaging modalities requiring 10–30 min response times, our method achieves rapid diagnosis within minutes post-sampling without complex instrumentation. Histopathological analysis confirmed Cy-PITC's biosafety, with no treatment-related tissue abnormalities observed (Fig. S18).

Following successful validation in murine models, we translated the Cy-PITC assay to clinical AKI diagnosis using human urine. We recruited 10 healthy individuals and 30 AKI patients, and their biochemical parameters are detailed in SI Table S3. The streamlined protocol (Fig. 5A) involves urine–Cy-PITC incubation (<2 min) and smartphone-based fluorescence

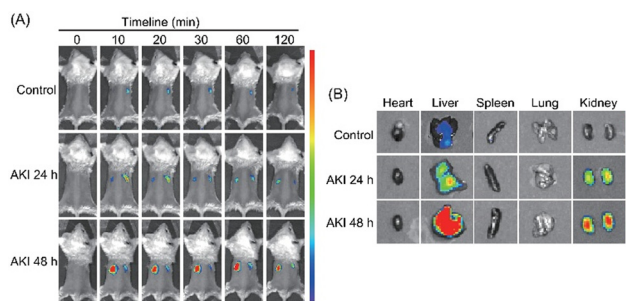


**Fig. 3** Representative NIRF images of living mice after i.v. injection of Cy-PITC at different post-cisplatin treatment time points (24 h and 48 h). (A) *In vivo* NIRF imaging of Cy-PITC in normal mice and cisplatin-induced AKI mice. (B) *Ex vivo* NIRF imaging of isolated organs, involving the heart, liver, spleen, lung, and kidneys.

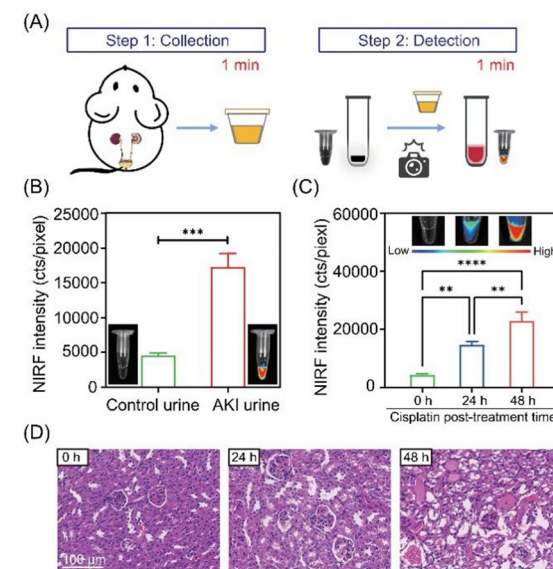


**Fig. 4** Urinalysis via NIRF in AKI mice. (A) Schematic representation of the application of Cy-PITC in urinalysis of drug-induced AKI mice. (B) Fluorescence image and NIRF intensity of urine incubated with 2  $\mu$ M Cy-PITC from control mice and AKI mice. (C) NIRF intensity and fluorescence image of urine incubated with 2  $\mu$ M Cy-PITC from cisplatin-treated mice at indicated post-injection time points (0, 24, and 48 h). (D) Photomicrographs of H&E staining of kidney sections from mice at different post-treatment time points. \*\* $P$  < 0.01, \*\*\*\* $P$  < 0.0001.



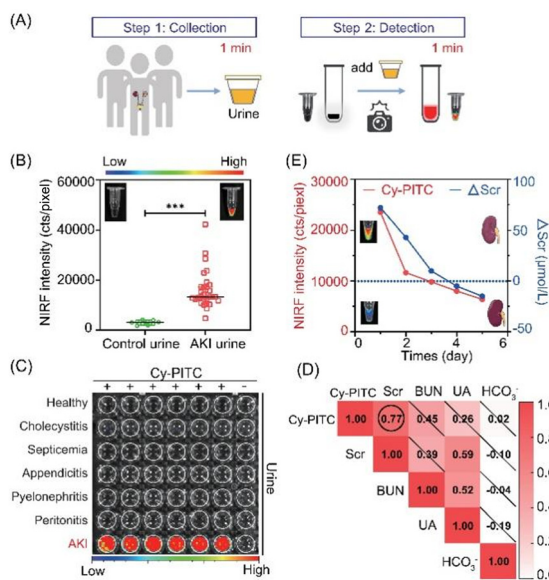


**Fig. 5** Urinalysis via NIRF in AKI patients. (A) Schematic representation of the application of Cy-PITC in urinalysis of AKI patients. (B) Fluorescence image and NIRF intensity distribution analysis (control urine  $n = 10$ , AKI urine  $n = 30$ ). (C) Fluorescence imaging of healthy individuals, AKI patients, and patients with other inflammatory diseases. (D) Correlation between Cy-PITC fluorescence intensity and renal function indexes. (E) The changes in serum creatinine levels ( $\Delta\text{Scr}$ ) and Cy-PITC NIRF fluorescence intensity over time. \*\*\* $P < 0.001$ .

imaging, enabling point-of-care testing. This approach could be easily integrated with a smartphone to produce a portable and miniaturized test device and facilitate the determination of urine biomarkers. Clinical analysis revealed a 5.4-fold fluorescence enhancement in AKI patients *versus* controls (Fig. 5B and S19). Notably, Cy-PITC selectively distinguished AKI patients from those with non-renal inflammatory diseases (*e.g.*, septicemia), showing higher fluorescence in AKI *versus* inflammatory controls (Fig. 5C), consistent with compartmentalized renal HClO production. Cy-PITC signals strongly correlated with Scr (Pearson's  $r = 0.77$ , Fig. 5D) but not hepatic/electrolyte markers (Fig. S20), confirming renal specificity. Longitudinal monitoring of a recovering AKI patient demonstrated parallel declines in  $\Delta\text{Scr}$  and urinary Cy-PITC intensity (Fig. 5E), reflecting real-time renal functional improvement. ROC analysis further validated high diagnostic accuracy (AUC = 1.0, Fig. S21), underscoring clinical utility.

In conclusion, we have successfully developed a sample-to-answer approach for AKI detection. Owing to the regioselective conversion of thioamide to amide in Cy-PITC, trace amounts of  $\text{ClO}^-/\text{HClO}$  in the urine of AKI patients could be easily lit up within 1 minute and captured using a camera. The urine-based analysis results were consistent with the results from standard clinical blood-based Scr assessments. Our technique does not require complex equipment and well-trained personnel. More importantly, the assay time was significantly reduced from several hours to just 1–2 minutes. This advancement has the potential to greatly enhance AKI diagnostics,

enabling both healthcare professionals and non-experts to make rapid, accurate decisions.

## Conflicts of interest

There are no conflicts to declare.

## Data availability

The data supporting this article have been included as part of the supplementary information (SI). Supplementary information including Materials and General Experimental Methods, Figure S1–S21, Table S1–S3, is available. See DOI: <https://doi.org/10.1039/d5an00859j>.

## Acknowledgements

This work was partially supported by National Key R&D Program of China (2023YFC3605500), the National Natural Science Foundation of China (82470719, 82460364), the Guangxi Natural Science Foundation (2025GXNSFAA069545), the Guangdong Basic and Applied Basic Research Fund Enterprise Joint Fund (2023A1515220119), the Doctoral Research Initiation Fund Project of GLNU(2025040809), and the Shenzhen Science and Technology Program (KQTD20210811090115019). All animal procedures were performed in accordance with the Guidelines for Care and Use of Laboratory Animals of “Peking” University and approved by the Animal Ethics Committee of “SHENZHEN PKU- HKUST MEDICALCENTER” (Approval number: 2024-549). All human-related experiments were performed in accordance with the Guidelines “1964 Helsinki Declaration” and its later amendments or comparable ethical standards’ and approved by the ethics committee at “The Second Affiliated Hospital of Shenzhen University” (Approval number: BYL20240471) Informed consents were obtained from human participants of this study.

## References

1. A. Vijayan, Tackling AKI: prevention, timing of dialysis and follow-up, *Nat. Rev. Nephrol.*, 2021, **17**(2), 87–88.
2. H. Lee, K. H. Liu, Y. H. Yang, *et al.*, Advances in uremic toxin detection and monitoring in the management of chronic kidney disease progression to end-stage renal disease, *Analyst*, 2024, **149**(10), 2784–2795.
3. Y. Wen and C. R. Parikh, Current concepts and advances in biomarkers of acute kidney injury, *Crit. Rev. Clin. Lab. Sci.*, 2021, **58**(5), 354–368.
4. E. Derin and F. Inci, Advances in Biosensor Technologies for Acute Kidney Injury, *ACS Sens.*, 2022, **7**(2), 358–385.
5. X. Xu, S. Nie, H. Xu, B. Liu, J. Weng, C. Chen, *et al.*, Detecting Neonatal AKI by Serum Cystatin C, *J. Am. Soc. Nephrol.*, 2023, **34**(7), 1253–1263.



6 A. Zhang, Y. Wang, X. Sui, *et al.*, Renal-Clearable Biomass-Derived Carbon Dots with Red Fluorescence for Masked Cryptic Kidney Injury Imaging, *ACS Appl. Bio. Mater.*, 2025, **8**(2), 1148–1156.

7 J. Wang, Z. J. Sheng, J. R. Guo, *et al.*, Near-Infrared Fluorescence Probes for Monitoring and Diagnosing Nephron-Urological Diseases, *Coord. Chem. Rev.*, 2023, **486**, 215137.

8 Z. W. Zhao, W. Xiang, W. T. Guo, *et al.*, A Dual-Channel Fluorescence Probe for Early Diagnosis and Treatment Monitoring of Acute Kidney Injury by Detecting HOCl and Cys with Different Fluorescence Signals, *Anal. Chem.*, 2025, **97**(4), 2127–2135.

9 P. Liu, Y. Zhao, Y. Peng, *et al.*, Harnessing the power of nanoagents in acute kidney injury: A versatile platform for imaging and treatment, *Coord. Chem. Rev.*, 2025, **533**, 216570.

10 L. Y. Tan, E. Liang, X. H. Zheng, *et al.*, Ultrasensitive chemiluminescent probe activated by NAG for real-time monitoring of AKI, *Bioorg. Chem.*, 2025, **164**, 108817.

11 J. Huang, X. Chen, Y. Jiang, C. Zhang, S. He, H. Wang, *et al.*, Renal clearable polyfluorophore nanosensors for early diagnosis of cancer and allograft rejection, *Nat. Mater.*, 2022, **21**(5), 598–607.

12 Y. Y. Kong, B. Liu, Y. H. Zhang, *et al.*, Coumarin-based fluorescent probe for hypochlorite detection and imaging of acute kidney injury, *Sens. Actuators, B*, 2025, **435**, 137645.

13 B. Zhao, X. Xu, X. Wen, *et al.*, Ratiometric Near-Infrared Fluorescent Probe Monitors Ferroptosis in HCC Cells by Imaging HClO in Mitochondria, *Anal. Chem.*, 2024, **96**(15), 5992–6000.

14 Q. Xu, K.-A. Lee, S. Lee, *et al.*, A Highly Specific Fluorescent Probe for Hypochlorous Acid and Its Application in Imaging Microbe-Induced HOCl Production, *J. Am. Chem. Soc.*, 2013, **135**(26), 9944–9949.

15 E. M. Worcester, K. J. Bergsland, D. L. Gillen and F. L. Coe, Mechanism for higher urine pH in normal women compared with men, *Am. J. Physiol. Renal Physiol.*, 2018, **314**(4), F623–F629.

16 S. Gupta, I. G. Glezerman, J. S. Hirsch, K. L. Chen, N. Devaraj, S. L. Wells, *et al.*, Derivation and external validation of a simple risk score for predicting severe acute kidney injury after intravenous cisplatin: cohort study, *Br. Med. J.*, 2024, **384**, e077169.

17 M. Baruah, A. Jana, M. Ali, *et al.*, An efficient PeT based fluorescent probe for mapping mitochondrial oxidative stress produced via the Nox2 pathway, *J. Mater. Chem. B*, 2022, **10**(13), 2230–2237.

18 H. L. Huang, N. Cheng, C. X. Zhou and J. Liang, Megalin-targeted acetylcysteine polymeric prodrug ameliorates ischemia-reperfusion-induced acute kidney injury, *Helijon*, 2024, **10**(10), e30947.

19 C. Ronco, R. Bellomo and J. A. Kellum, Acute kidney injury, *Lancet*, 2019, **394**(10212), 1949–1964.